

Syntheses, crystal structures and photophysical properties of d^{10} transition-metal (Ag^+ , Cu^+ , Cd^{2+} and Zn^{2+}) coordination complexes based on a thiophene-containing heterocyclic thioamide

Yu-Zhen Wei, Zheng Cheng, Wei Li & Hai-Bin Zhu

To cite this article: Yu-Zhen Wei, Zheng Cheng, Wei Li & Hai-Bin Zhu (2017): Syntheses, crystal structures and photophysical properties of d^{10} transition-metal (Ag^+ , Cu^+ , Cd^{2+} and Zn^{2+}) coordination complexes based on a thiophene-containing heterocyclic thioamide, Journal of Coordination Chemistry, DOI: [10.1080/00958972.2017.1364374](https://doi.org/10.1080/00958972.2017.1364374)

To link to this article: <http://dx.doi.org/10.1080/00958972.2017.1364374>

 View supplementary material 

 Accepted author version posted online: 04 Aug 2017.
Published online: 16 Aug 2017.

 Submit your article to this journal 

 Article views: 2

 View related articles 

 View Crossmark data 



Syntheses, crystal structures and photophysical properties of d¹⁰ transition-metal (Ag⁺, Cu⁺, Cd²⁺ and Zn²⁺) coordination complexes based on a thiophene-containing heterocyclic thioamide

Yu-Zhen Wei^a, Zheng Cheng^b, Wei Li^b  and Hai-Bin Zhu^a

^aSchool of Chemistry and Chemical Engineering, Southeast University, Nanjing, China; ^bSchool of Chemistry and Chemical Engineering, Nanjing University, Nanjing, China

ABSTRACT

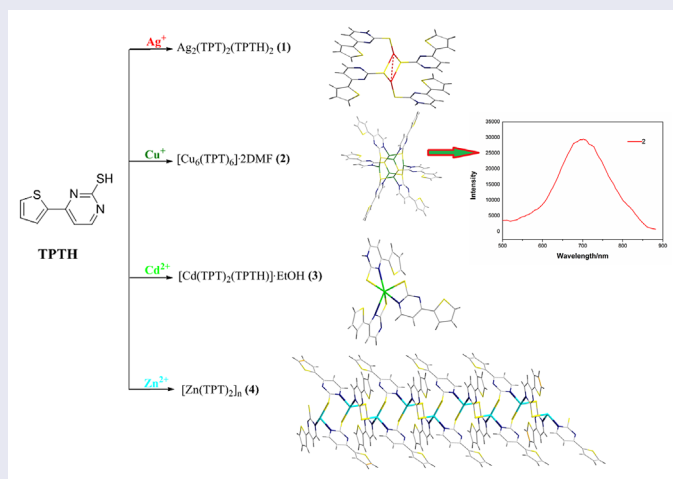
Four d¹⁰ transition-metal coordination complexes **1–4** (**1**: [Ag₂(TPT)₂(TPTH)₂]_n; **2**: [Cu₆(TPT)₆]-2DMF; **3**: [Cd(TPT)₂(TPTH)]-CH₃CH₂OH, **4**: [Zn(TPT)₂]_n) have been constructed from a newly designed heterocyclic thioamide ligand, TPTH (TPTH = 4-(thiophen-2-yl)-pyrimidine-2-thiol). All complexes have been structurally elucidated by single crystal X-ray diffraction analyses. Except for **4**, which shows a one-dimensional (1-D) chain structure, **1–3** are all discrete coordination complexes featuring dinuclear, hexanuclear and mononuclear entities, respectively. Their photophysical properties have been evaluated in the solid state at room temperature by UV–vis diffuse reflectance and luminescence spectra. Among them, **2** exhibits a strong red luminescence (λ_{em} = 699 nm) with a remarkable red-shift of the maximum emission compared to that of the TPTH ligand (λ_{em} = 536 nm). The red emission observed with **2** is ascribed to a LMCT (ligand-to-metal charge transfer) transition which agrees with the DFT calculations.

ARTICLE HISTORY

Received 20 February 2017
Accepted 10 July 2017

KEYWORDS

d¹⁰ Transition-metal;
heterocyclic thioamide;
crystal structures;
photophysical properties



CONTACT Hai-Bin Zhu  zhuhabin@seu.edu.cn

 Supplemental data for this article can be accessed at <https://doi.org/10.1080/00958972.2017.1364374>.

© 2017 Informa UK Limited, trading as Taylor & Francis Group

1. Introduction

Owing to their rich coordination chemistry, there is a long-standing interest in heterocyclic thioamide (HTA) ligands [1–13]. All sorts of coordination modes with heterocyclic thioamides have been well summarized in two earlier excellent reviews [12, 13]. They can behave either as unidentate or multidentate ligand, binding metal centers via exocyclic sulfur and/or heterocyclic nitrogen atoms [14–20]. Besides, the $\text{-N(H)-C(=S)} \leftrightarrow \text{-N=C(-SH)-}$ tautomerization with heterocyclic thioamides provides an interesting structural variant that would add more uncertainties into the final metal-coordination structures [6, 21, 22].

As the simplest member of the HTA family, pyrimidine-2-thiol (pymtH) as well as its substituted derivatives have been extensively studied [10, 16, 19, 20, 23–28]. As demonstrated by these preceding works, the introduction of different substituents onto pymtH might prevent the rapid formation of polymeric precipitates as the result of an increase in steric hindrance. In our previous research, we have reported one class of substituted pymtH ligands ($n\text{-PPT}$, $n = 2, 3, 4$) that couples one coordinative pyridine group at its C-4 site [10, 29, 30]. In continuation of our previous work, herein we have designed a new 4-substituted pymtH ligand, TPTH (TPTH=4-(thiophen-2-yl)-pyrimidine-2-thiol), that incorporates a thiophene unit (Scheme 1). The introduction of a thiophene substituent may favor the formation of discrete oligonuclear complexes with the TPTH ligand, owing to its hindering effect. More importantly, the conjugation of the electron-rich thiophene to the electron-deficient pyrimidine ring may induce a push–pull effect which is expected to have great influence on the photophysical properties of the resultant coordination complexes with the TPTH ligand.

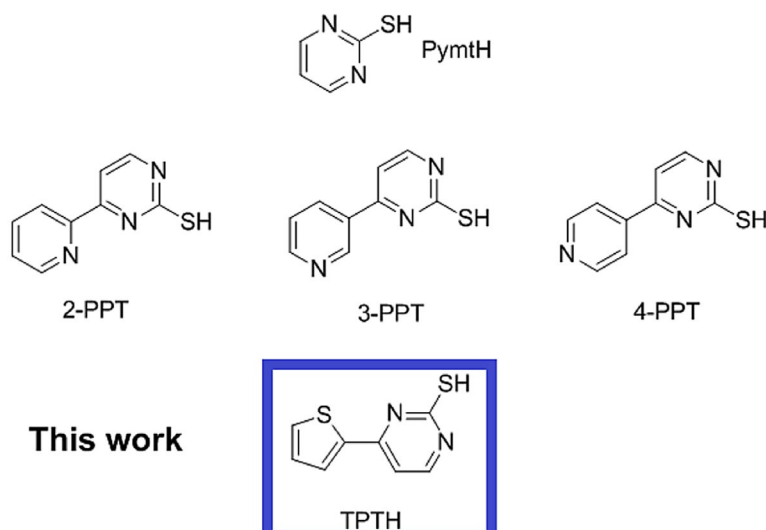
Coordination complexes based on transition metal ions with a d^{10} closed-shell electronic configuration have attracted attention largely not only because of their catalytic and biological properties, but also because of their intriguing photophysical properties [31–41], which have found wide applications such as emissive materials, imaging probes, and photocatalysts. In this context, d^{10} transition-metal complexes with heterocyclic thioamides have been reported to display interesting photoluminescence properties [7, 16, 42, 43], possibly because the thiolate-S bridged metal centers may establish super-exchange interactions between them through spin density delocalization toward the bridging S atom in the case that the selected metal orbital energies are better matched for the sulfur atom.

For the aforementioned reasons, we have prepared four d^{10} metal-ion-based (Ag^+ , Cu^+ , Cd^{2+} , Zn^{2+}) coordination complexes (**1–4**) with TPTH ligand in this work and studied the correlation between their crystal structures and photophysical properties.

2. Experimental

2.1. Materials and measurements

All chemicals were of analytical grade and used as received. The reagents for synthesis of the TPTH ligand including 2-acetylthiophene, N,N' -dimethylformamide dimethylacetal, and thiourea were obtained from J&K China Chemical Ltd. Metal salts for preparation of coordination complexes **1–4** including AgNO_3 , $\text{Cu}(\text{NO}_3)_2 \cdot 3\text{H}_2\text{O}$, $\text{Cd}(\text{ClO}_4)_2 \cdot 6\text{H}_2\text{O}$, and $\text{Zn}(\text{ClO}_4)_2 \cdot 6\text{H}_2\text{O}$ were all purchased from Sinopharm Chemical Reagent Co., Ltd. (China). IR spectra were recorded with a Thermo Scientific Nicolet 5700 FT-IR spectrophotometer as KBr pellets from 400 to 4000 cm^{-1} . ^1H NMR spectra were recorded with a Bruker AVANCE-500 spectrometer. Powder X-ray diffraction (PXRD) data were collected on an XRD diffractometer (D8 Discover,



Scheme 1. Schematic representation of N-heterocyclic thioamide ligands of PymtH and n-PPT ($n = 2, 3,$ and 4).

Bruker-AXS) with Cu- $K\alpha$ radiation ($\lambda = 1.54056 \text{ \AA}$). The UV-vis diffuse-reflectance spectra of samples of **1–4** were recorded on a Shimadzu UV-2450 spectrophotometer equipped with an integrating sphere and using BaSO_4 as the reference. The luminescence spectra were measured via fluorescent spectra (Horiba Fluoromax4 spectrometer) using a Xe lamp as the excitation source at room temperature.

2.2. Computational details

The cluster structure of **2** was obtained from its crystal structure, and the lowest excitation state of **2** was obtained by time-dependent density functional theory (TDDFT) calculations with the Austin-Frisch-Petersson function with dispersion (APFD) and the 6-31G(d) basis set [44]. All the TDDFT calculations were carried out using the Gaussian 09 package [45].

2.3. Synthesis of 4-(thiophen-2-yl)pyrimidine-2-thiol (TPTH)

2-Acetylthiophene (3.80 g, 30.0 mmol) and N,N-dimethylformamide dimethylacetal (3.95 g, 33.1 mmol) were added to 50 mL of DMF (DMF=N,N-dimethylformamide). The mixture was stirred under reflux for 7 h. Upon cooling to room temperature, the solution was concentrated by rotatory evaporation to give a semisolid which was further washed with ether and dried under vacuum to afford intermediate P1 ((Z)-3-(dimethylamino)-1-(thiophen-2-yl)prop-2-en-1-one) as a yellow solid powder and the yield was 87% (Calcd, 5.46 g).

0.6 g (26.0 mmol) of sodium was added into 50 mL of absolute ethanol at room temperature. After the sodium was completely consumed, 2.50 g (13.8 mmol) of P1 and 1.30 g (17.1 mmol) of thiourea were added into the above solution, and the reaction mixture was then refluxed for 6 h. Upon cooling to room temperature, the reaction mixture was adjusted to pH = 6–7 with 2 M HCl which resulted in TPTH (4-(thiophen-2-yl)pyrimidine-2-thiol) as a yellow precipitate, which was washed with water and dried under vacuum. Yield: 76% (Calcd,

2.68 g). IR (KBr, cm^{-1}): 1605 (s), 1560 (s), 1523 (w), 1468 (s), 1417 (w), 1398 (w), 1253 (s), 1226 (w), 1204 (w), 1170 (s), 971 (w), 799 (w), 713 (w). ^1H NMR (d_6 -DMSO/TMS, 500 MHz, ppm): δ 13.50 (s, 1H), 8.02 (s, 1H), 8.00 (s, 2H), 7.35 (d, 2H). ESI-MS: $m/z = 195.00$ [$\text{M} + \text{H}^+$] $^+$ (100%). Anal. Calcd for $\text{C}_8\text{H}_6\text{N}_2\text{S}_2$ (%): C, 49.45; H, 3.11; N, 14.42. Found: C, 49.32; H, 3.01; N, 14.31.

2.4. Synthesis of complexes 1–4

2.4.1. Synthesis of $[\text{Ag}_2(\text{TPT})_2(\text{TPTH})_2]\{\text{bis}(4\text{-}(\text{thiophen-2-yl})\text{pyrimidine-2-thiolate})\text{bis}(4\text{-}(\text{thiophen-2-yl})\text{pyrimidine-2(1H)-thione})\text{disilver(I)}\}$ (1)

A methanol solution (3 mL) of AgNO_3 (4.25 mg, 0.025 mmol) was carefully layered above a DMF solution (1 mL) of TPTH (9.71 mg, 0.05 mmol). Bulk orange block crystals were obtained after 1–2 weeks. The orange crystals of **1** were collected and dried under vacuum. Single crystals suitable for X-ray diffraction analysis were selected from the crystals (yield: 4.43 mg, 35% based on TPTH). IR (KBr, cm^{-1}): 1610 (w), 1559 (s), 1519 (w), 1404 (s), 1355 (w), 1312 (w), 1266 (s), 1228 (w), 1189 (s), 1095 (w), 806 (w), 716 (w). Anal. Calcd for $\text{C}_{32}\text{H}_{22}\text{Ag}_2\text{N}_8\text{S}_8$ (%): C, 38.79; H, 2.23; N, 11.31. Found: C, 38.65; H, 2.12; N, 11.19.

2.4.2. Synthesis of $[\text{Cu}_6(\text{TPT})_6]\cdot 2\text{DMF}\{\text{hexa}(4\text{-}(\text{thiophen-2-yl})\text{pyrimidine-2-thiolate})\text{hexacopper(II) dimethylformamide disolvate}\}$ (2)

A methanol solution (5 mL) of $\text{Cu}(\text{NO}_3)_2\cdot 3\text{H}_2\text{O}$ (24.1 mg, 0.1 mmol) was carefully layered above a DMF solution (1 mL) of TPTH (9.71 mg, 0.05 mmol). Bulk red block crystals of **2** were obtained after 2–3 weeks by slow evaporation at room temperature (yield: 5.81 mg, 27% based on TPTH). IR (KBr, cm^{-1}): 1665 (w), 1565 (s), 1535 (w), 1518 (w), 1426 (w), 1400 (w), 1356 (w), 1322 (s), 1165 (w), 1092 (w), 821 (w), 793 (w), 715 (w). Anal. Calcd for $\text{C}_{54}\text{H}_{44}\text{Cu}_6\text{O}_2\text{N}_{14}\text{S}_{12}$ (%): C, 38.44; H, 2.63; N, 11.63. Found: C, 38.31; H, 2.50; N, 11.52.

2.4.3. Synthesis of $[\text{Cd}(\text{TPT})_2(\text{TPTH})_2]\cdot \text{CH}_3\text{CH}_2\text{OH}\{\text{bis}(4\text{-}(\text{thiophen-2-yl})\text{pyrimidine-2-thiolate})\text{(4-}(\text{thiophen-2-yl})\text{pyrimidine-2(1H)-thione})\text{cadmium(II) ethanol solvate}\}$ (3)

An ethanol solution (3 mL) of $\text{Cd}(\text{ClO}_4)_2\cdot 6\text{H}_2\text{O}$ (10.48 mg, 0.025 mmol) was carefully layered above a DMF solution (1 mL) of TPTH (9.71 mg, 0.05 mmol). Bulk yellow block crystals of **3** were obtained after 3–4 weeks (yield: 3.39 mg, 27% based on TPTH). IR (KBr, cm^{-1}): 1672 (w), 1617 (w), 1561 (s), 1427 (w), 1403 (w), 1362 (s), 1334 (w), 1168 (w), 1111 (w), 814 (w), 785 (w), 720 (w). Anal. Calcd for $\text{C}_{26}\text{H}_{22}\text{CdON}_6\text{S}_6$ (%): C, 42.24; H, 3.00; N, 11.37. Found: C, 42.12; H, 2.89; N, 11.23.

2.4.4. Synthesis of $[\text{Zn}(\text{TPT})_2]_n\{\text{poly-}[\text{bis}(4\text{-}(\text{thiophen-2-yl})\text{pyrimidine-2-thiolate})\text{zinc(II)}]\}$ (4)

$\text{Zn}(\text{ClO}_4)_2\cdot 6\text{H}_2\text{O}$ (9.31 mg, 0.025 mmol) and TPTH (9.71 mg, 0.05 mmol) in the H_2O -DMF mixture solution (v:v = 3:1, 4 mL) was added to a Teflon-lined autoclave (23 mL) and heated at 120° for 72 h affording as a single phase, yellow block-shaped crystals of **4**, which were filtered, washed with DMF and dried under vacuum (yield: 2.65 mg, 23% based on TPTH). IR (KBr, cm^{-1}): 1610 (w), 1559 (s), 1519 (w), 1419 (w), 1404 (s), 1312 (w), 1266 (s), 1228 (w), 1189 (s), 1167 (w), 806 (w), 732 (w), 716 (w). Anal. Calcd for $\text{C}_{16}\text{H}_{10}\text{ZnN}_4\text{S}_4$ (%): C, 42.52; H, 2.23; N, 12.40. Found: C, 42.41; H, 2.12; N, 12.31.

2.5. X-ray crystallography

Diffraction intensity data for **1–4** were collected at 298(2) K with a Bruker SMART CCD-4 K diffractometer by employing graphite-monochromated MoK α radiation ($\lambda = 0.71073 \text{ \AA}$). The data were collected using SMART and reduced using SAINT [46]. A semi-empirical absorption correction was applied using SADABS [47]. All the structures were solved by direct methods and refined by full-matrix least squares methods on F^2_{obs} using the SHELXTL-97 crystallographic software package [48]. All non-hydrogen atoms were refined anisotropically. All hydrogens were calculated by geometrical methods and refined as a riding model. The crystallographic data of **1–4** are presented in Table 1. The selected bond lengths and angles of **1**, **3** and **4** are summarized in Table 2. The selected bond lengths and angles of **2** are summarized separately in Table S1. The bond lengths and angles of the hydrogen bonds in **1–4** are listed in Table S2.

3. Results and discussion

3.1. Synthetic procedure for TPTH

The synthetic procedure for TPTH was developed on the basis of our previous work [49–51]. As outlined in Scheme 2, the title organic molecule, TPTH, was prepared in two steps. In the first step, the aldol condensation of 2-acetylthiophene with N,N-dimethylformamide dimethylacetal almost quantitatively produced the P1 intermediate. In the second step, the installation of the pyrimidinylthiol moiety of the TPTH ligand was accomplished by reaction of P1 with thiourea under basic conditions. The molecular structure of TPTH was confirmed by ^1H NMR, ESI-MS and elemental analysis. The ^1H NMR spectrum of TPTH in d_6 -DMSO shows a singlet for the pyrimidine protons at $\delta = 8.00$ ppm, two resonances at $\delta = 7.31$ and 8.20 ppm corresponding to thiophene protons, and one signal at $\delta = 13.50$ ppm from the -SH proton (Figure S1). The ESI-MS spectra of TPTH exhibits a signal at $m/z = 195.00$, which agrees well with the formula weight of TPTH.

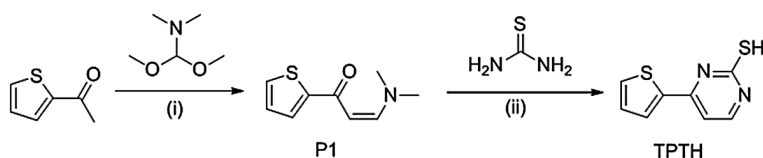
Table 1. Crystallographic data for **1–4**.

Complex	1	2	3	4
Formula	$\text{C}_{32}\text{H}_{22}\text{Ag}_3\text{N}_8\text{S}_8$	$\text{C}_{54}\text{H}_{44}\text{Cu}_2\text{O}_2\text{N}_{14}\text{S}_{12}$	$\text{C}_{26}\text{H}_{22}\text{CdON}_6\text{S}_6$	$\text{C}_{16}\text{H}_{10}\text{ZnN}_4\text{S}_4$
Formula weight	990.80	1686.99	739.26	451.91
Crystal system	Monoclinic	Monoclinic	Triclinic	Monoclinic
Space group	C2/c	C2/c	$\bar{P}1$	C2/c
a (Å)	17.504(4)	29.515(4)	9.759(3)	26.307(17)
b (Å)	11.645(2)	11.3462(15)	10.248(3)	7.007(5)
c (Å)	18.063(4)	20.503(3)	17.137(4)	19.582(13)
α (°)	90.00	90.00	100.102(4)	90.00
β (°)	106.53(3)	106.398(2)	90.353(4)	99.626(8)
γ (°)	90.00	90.00	109.747(4)	90.00
V (Å 3)	3529.9(12)	6586.8(16)	1584.1(7)	3559(4)
Z	4	4	2	8
D_{calc} (g cm $^{-3}$)	1.865	1.701	1.550	1.687
$F(000)$	1968	3392	744	1824
Reflections collected	20,384	22,943	8778	11,598
Unique reflections	5862	5809	5539	3077
R_{int}	0.031	0.043	0.020	0.052
R_1, wR_2 [$> 2\sigma(I)$]	0.0388/0.1093	0.0403/0.1092	0.0404/0.1163	0.0463/0.1411
R_1, wR_2 (all data)	0.0452/0.1154	0.0546/0.1158	0.0518/0.1229	0.0518/0.1491
Goodness-of-fit	1.05	1.08	1.03	1.04

$$R_1 = \frac{\sum ||F_o| - |F_c||}{\sum |F_o|}, wR_2 = \frac{|\sum w(|F_o|^2 - |F_c|^2)|}{\sum w(F_o)^2}^{1/2}, \text{ where } w = 1/[\sigma^2(F_o^2) + (aP)^2 + bP]. P = (F_o^2 + 2F_c^2)/3.$$

Table 2. Selected bond lengths (Å) and angles (°) for **1**, **3**, and **4**.

1		3		4	
<i>Bond lengths</i>					
Ag1-S3	2.4426(8)	Cd1-S2	2.595(1)	Zn1-N1A	2.053(4)
Ag1-S1	2.4802(9)	Cd1-S4	2.515(1)	Zn1-N3B	2.102(4)
Ag1-S3A	2.9117(9)	Cd1-S6	2.483(1)	Zn1-S3	2.3356(16)
Ag1-Ag1A	3.0872(7)	Cd1-N2	2.458(3)	Zn1-S2	2.4048(15)
S1-C1	1.705(2)	Cd1-N4	2.780(3)	S2-C8	1.733(4)
S3-C9	1.744(2)	Cd1-N6	2.769(4)	S3-C16	1.752(4)
		S2-C8	1.738(4)		
		S6-C24	1.722(4)		
		S4-C16	1.723(4)		
<i>Bond angles</i>					
S3-Ag1-S3A	110.21(2)	N2-Cd1-S2	62.29(9)	N1A-Zn1-N3B	97.51(14)
N4-C9-S3	117.85(16)	N4-Cd1-S4	60.13(7)	N1A-Zn1-S3	144.62(11)
N1-C1-S1	118.77(18)	N6-Cd1-S6	60.37(7)	N3B-Zn1-S3	100.67(10)
		N2-Cd1-N	676.6(1)	N1A-Zn1-S2	102.46(10)
		N2-C8-S2	115.6(3)	N1-C8-S2	115.3(3)
		N4-C16-S4	120.1(3)	N3-C16-S3	116.1(3)
		N6-C24-S6	118.2(3)		

**Scheme 2.** Synthesis of TPTH.

Apart from **4**, afforded by a solvothermal reaction, the complexes were all obtained by a slow diffusion method using dilute solutions in order to control the reaction rate. Crystal structures of **1–4** have been further ascertained by single-crystal X-ray diffraction analysis (*vide infra*). The phase purity of the as-synthesized samples of **1–4** was confirmed by the consistency between the experimental PXRD pattern and the simulated PXRD pattern (Figure S2).

3.2. Crystal structure of $[Ag_2(TPT)_2(TPTH)_2]$ (**1**)

Single crystal X-ray crystallography reveals that **1** crystallizes in the monoclinic space group $C2/c$ with the asymmetric unit comprising one Ag atom and two independent TPTH ligands (Figure S3). As shown in Figure 1, **1** shows a discrete binuclear structure composed of two Ag atoms and four TPTH ligands that are related by a symmetry center. The Ag (I) center is three-coordinate by three S atoms from three ligands, and the Ag-S bond distances (Ag1-S1: 2.4802(9) Å, Ag1-S3A: 2.9117(9) Å, Ag1-S3: 2.4426(8) Å) are comparable to those reported for silver complexes with pyridine-2-thiolate and pyrimidine-2-thiolate derivatives [19, 52–55]. Interestingly, there exist two forms of TPTH ligands in a 1:1 ratio, *viz.* thiolate anion and neutral thione (Figure S4), which differ in their C-S bond lengths (C-S bond of thiolate: 1.744(2) Å; C-S bond of neutral thione: 1.705(2) Å). The former is connected to two Ag atoms through a single thiolate-S atom, and the latter is terminally bonded to one Ag atom through the thione-S atom. Two Ag atoms and two thiolate-S atoms build a Ag_2S_2 parallelogram

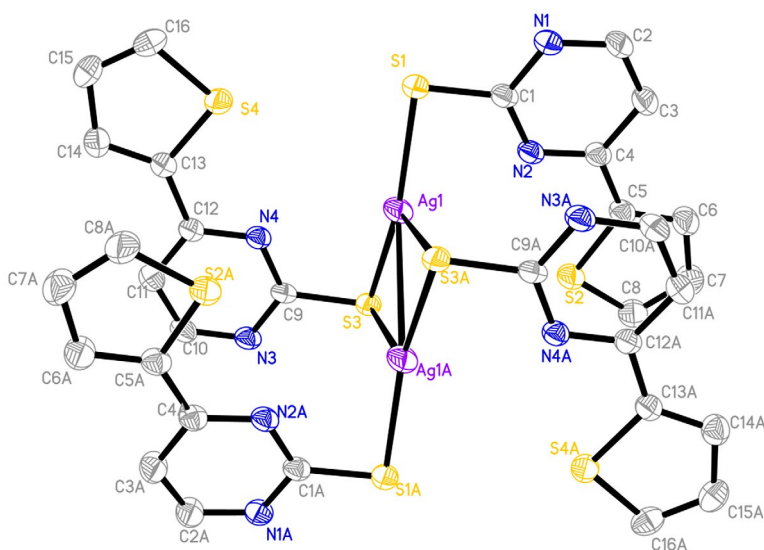


Figure 1. ORTEP view of **1** drawn at the 50% probability level (hydrogens omitted for clarity; symmetry code: (A) $-x + 1/2, -y + 1/2, -z + 1$).

(Ag1-S3A: 2.9117(9) Å, Ag1A-S3A: 2.4426(8) Å, S3-Ag1-S3A: 110.21(2)°, Ag1-S3A-Ag1A: 69.79(1)°). With reference to the Ag_2S_2 parallelogram, four TPTH ligands are alternate arranged in *cis*- and *trans*-conformations. The $\text{Ag}\cdots\text{Ag}$ distance of 3.0872(7) Å is much shorter than the sum of the *van der Waals* radii (3.44 Å), which falls into the range of 2.89–3.15 Å found in the reported Ag clusters with strong $\text{Ag}\cdots\text{Ag}$ interactions [56, 57]. The binuclear Ag entities of **1** are adhered to each other through N–H \cdots N hydrogen bonds (N–H \cdots N: 2.768(3) Å) between two forms of TPTH ligands and form a 1-D supramolecular chain (Figure S5a). More interestingly, the adjacent 1-D chains form a 2-D honeycomb supramolecular network via π – π stacking between the pyrimidine ring and the thiophene ring (Figure S5b).

3.3. Crystal structure of $[\text{Cu}_6(\text{TPT})_6]\cdot 2\text{DMF}$ (**2**)

Single crystal X-ray crystallography indicates that **2** crystallizes in the monoclinic space group $C2/c$ with the asymmetric unit comprising three copper(I) atoms, three TPTH ligands and one DMF guest molecule (Figure S6). As depicted in Figure 2, **2** shows a discrete centrosymmetric hexanuclear structure comprising six TPTH ligands and six Cu(I) atoms; the O atom of the guest DMF solvent is 5.379(4) Å away from Cu3. The Cu(I) atom resulted from *in situ* reduction of Cu(II) ion during the assembly reaction [16, 40, 58–60]. Each Cu(I) atom is trigonally coordinated to one nitrogen and two sulfur atoms from three different TPTH ligands with bond distances (Cu–S: 2.230(1) Å and 2.266(1) Å, Cu–N: 2.019(3) Å and 2.050(2) Å) being close to those copper(I) complexes with derivatives of heterocyclic-2-thiolates and heterocyclic-4-thiolates [58, 59, 61–66]. Different from **1**, the TPTH ligand in **2** only exist as thiolate anion, each linking three copper atoms in $\mu_3\text{-N}_{\text{exo}}\ \kappa^1\text{:S}, \kappa^2$ coordination fashion. The overall shape of **2** looks like a molecular paddlewheel in which six Cu(I) atoms form a distorted octahedron with Cu \cdots Cu separations in the range of 2.7377(7)–4.1995(8) Å (Figure S7), and each ligand linking three Cu(I) atoms defines one of the faces of this octahedron. It resembles

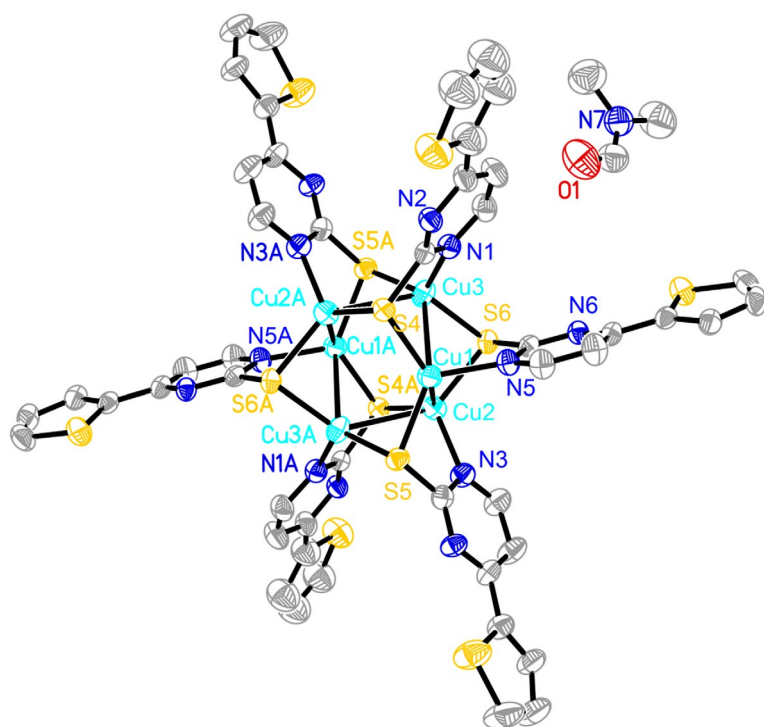


Figure 2. ORTEP view of **2** drawn at the 50% probability level (hydrogens omitted for clarity; symmetry code: (A) $-x + 1/2, -y + 1/2, -z$).

in structure the reported hexanuclear Cu(I) clusters with derivatives of pyridine-2-thiolate and pyrimidine-2-thiolate [67–74]. In the packing structure, complex **2** hexamers are further associated to each other through C–H \cdots O (3.526(7) Å) and C–H \cdots N (3.523(5) Å) hydrogen bonds (Figure S8).

3.4. Crystal structure of $[\text{Cd}(\text{TPT})_2(\text{TPTH})]\cdot\text{CH}_3\text{CH}_2\text{OH}$ (**3**)

Single-crystal X-ray crystallography shows that **3** crystallizes in the triclinic crystal system and $P\bar{1}$ space group and is composed of a discrete mononuclear Cd(II) coordination entity and one ethanol guest molecule. The six-coordinate Cd(II) atom in **3** is bound by three groups of N,S-chelating sets from three individual TPTH ligands, and the O atom of the guest ethanol solvent molecule is 7.84(1) Å from the Cd1 atom (Figure 3). Similar to **1**, **3** also possesses two forms of TPTH ligands, *viz.* thiolate anion (C–S bond: 1.737(4) Å) and neutral thione (C–S bond: 1.723(4) Å), but the thiolate anion/neutral thione ratio is 2:1 instead of 1:1. More interestingly, two TPTH thiolate anions are also distinct from each other regarding the coordinated N atom, wherein one is based on the *endo*-pyrimidine-N atom and the other on the *exo*-pyrimidine-N atom. In this aspect, the Cd(II) atom in **3** is actually bound by three types of TPTH ligands which is quite uncommon as far as we know. The Cd–S distances range from 2.483(1) Å to 2.595(1) Å, and the Cd–N distances are between 2.458(3) and 2.780(3) Å. The N–Cd–S angles lie within a very compact span of 60.13(7)–62.29(9)°. Finally, the mononuclear entities of **3**

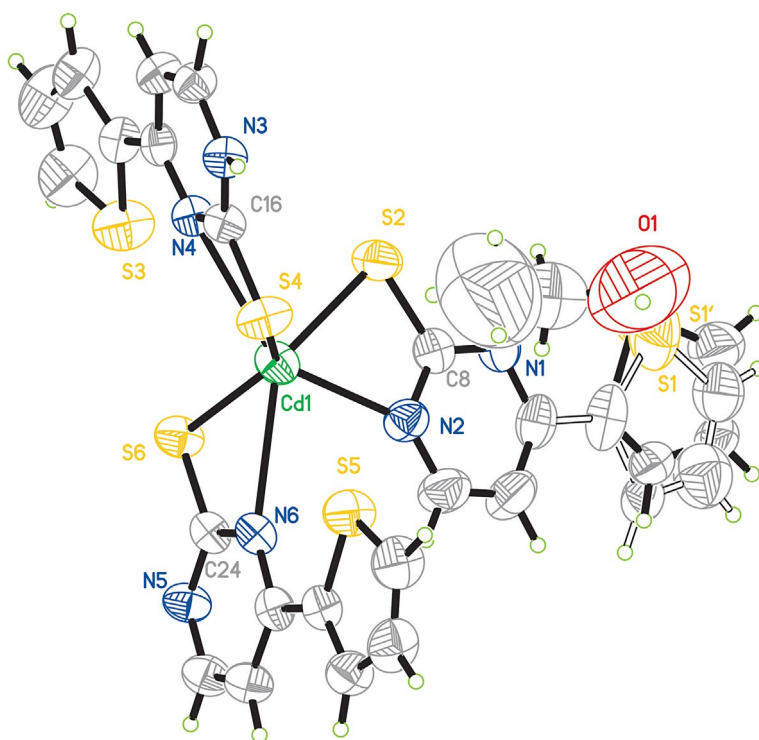


Figure 3. ORTEP view of **3** drawn at the 50% probability level.

are linked to each other through intermolecular N–H \cdots N (2.825(5) Å) hydrogen bonds, leading to formation of a 1-D chain structure (Figure S9).

3.5. Crystal structure of $[Zn(TPT)_2]_n$ (**4**)

X-ray crystallography reveals that **4** crystallizes in the monoclinic crystal system and $C2/c$ space group. The asymmetric unit of **4** consists of one Zn atom and two TPTH ligands (Figure S10). The Zn(II) atom in **4** adopts a distorted tetrahedral coordination geometry defined by two nitrogen atoms and two sulfur atoms belonging to four individual TPTH ligands (Figure 4(a)). All TPTH ligands in **4** are thiolate anions, each linking two Zn(II) atoms in a μ_2 -N_{exo}, κ^1 : S, κ^1 bridging mode (Zn1–S2: 2.405(2) Å; Zn–S3: 2.336(2) Å; Zn–N1A: 2.053(4) Å; Zn–N3B: 2.102(3) Å). Unlike the discrete structures of **1–3**, **4** shows a 1-D polymeric chain structure along the *b* axis that is built from adjacent Zn atoms doubly bridged by two TPTH ligands (the Zn \cdots Zn distance is 3.982(3) Å) (Figure 4(b)). Moreover, adjacent 1-D chains are connected by $\pi\cdots\pi$ stacking interactions between thiophene rings to give a 2-D layered structure (Figure S11).

3.6. Coordination modes of TPTH ligand in **1–4**

As demonstrated by **1–3**, the TPTH ligand favors the formation of discrete rather than polymeric coordination structures under ambient conditions, which can be attributed to the presence of non-coordinative thiophene groups that increase the steric hindrance for metal

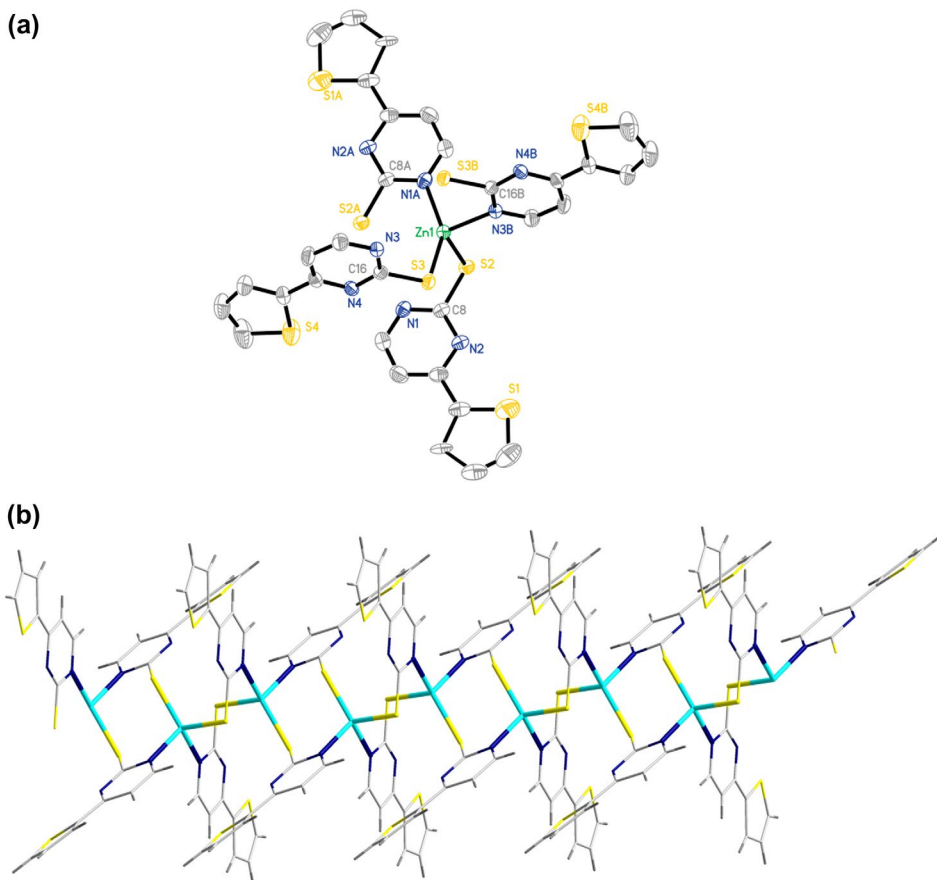
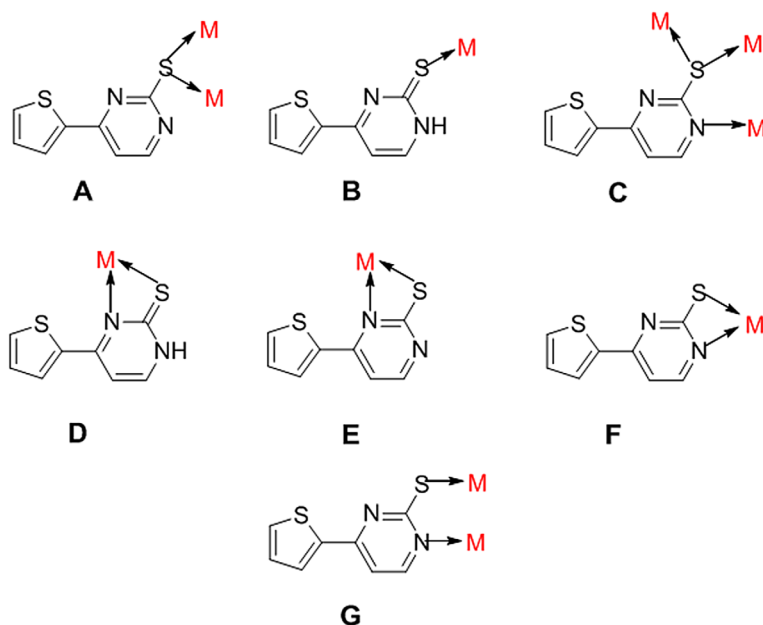


Figure 4. (a) ORTEP showing coordination environment of Zn atom of **4** drawn at the 50% probability (hydrogens omitted for clarity; symmetry codes: (A) $-x + 1/2, -y + 3/2, -z$; (B) $-x + 1/2, y + 5/2, -z$); (b) 1-D chain structure of **4**.

coordination. By contrast, the generation of 1-D Zn(II)-based polymeric coordination chains of **4** under solvothermal conditions might be the thermodynamic-driven product. Despite the non-coordinative nature of the thiophene substituent, TPTH exhibits versatile coordination modes (A-G) (Scheme 3). It may singly use an S atom as coordination donor either in the form of thiolate (A) or thione (B), or adopt mixed S, N-coordination (C, D, E, F, and G). In summary, coordination modes A and B in **1**, single coordination mode C in **2**; coordination modes D, E and F in **3**, and coordination mode G in **4** have been found.

3.7. Photophysical properties of 1–4

As shown in Figure 5(a), the absorption edge ($\lambda = 537$ nm) of TPTH is obviously extended toward long wavelength compared to the pymtH ($\lambda = 504$ nm), which can be accounted for by two factors pertinent to the thiophene substituent. On the one hand, the electron-rich nature of the thiophene substituent can raise the HOMO energy level with concomitant reduction of the HOMO–LUMO band gap. On the other hand, the introduction of the conjugated thiophene substituent facilitates the electron delocalization which also contributes



Scheme 3. The coordination modes of TPTH observed in 1–4.

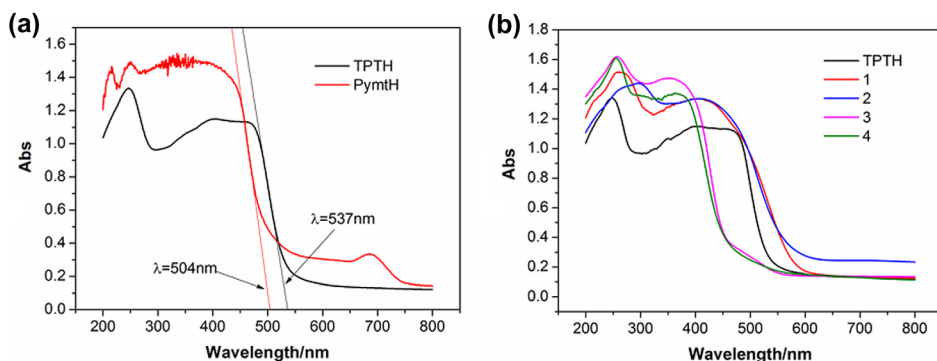


Figure 5. (a) Solid UV–vis absorption spectra of (a) TPTH and PymthH, (b) 1–4.

to the lower energy absorption. As depicted in Figure 5(b), the solid-state UV–vis absorption spectra of 1–4 resemble in shape that of the TPTH ligand, all being characterized by a narrow absorption band in the 204–300 nm region and a broad band in the 300–500 nm region, respectively. Accordingly, the UV–vis absorption properties of 1–4 can be attributed to the intraligand transitions of the TPTH ligand, wherein the absorption between 204–300 nm could be assigned to a $\pi \rightarrow \pi^*$ transition, and that in the 300–500 nm range to an $n \rightarrow \pi^*$ transition. Compared to the TPTH ligand, an obvious red-shift in the $\pi \rightarrow \pi^*$ absorption maximum is observed for 1 and 2 ($\lambda = 248$ nm for ligand, $\lambda = 266$ nm for 1, $\lambda = 295$ nm for 2) and slightly blue-shift for 3 and 4 ($\lambda = 258$ nm for 3 and $\lambda = 254$ nm for 4). Compared to TPTH, the $n \rightarrow \pi^*$ absorption band is slightly broadened in 1 and 2, but apparently narrowed for 3 and 4. Finally, a further extension of the absorption edge (1: 587 nm, 2: 591 nm) toward longer

wavelength is observed for **1** and **2** (Figure S12) compared to that of TPTH ligand, indicating that coordination to Ag⁺/Cu⁺ further narrows the optical band gap of TPTH. By contrast, the absorption edges of **3** and **4** are shifted remarkably toward shorter wavelength, inferring that the optical band gap is broadened upon coordination of TPTH to Zn²⁺/Cd²⁺ ion.

Figure 6(a) shows the emission spectra of **1–4** and the free TPTH ligand, which exhibits emission peaks at 569 nm, 699 nm, 465 nm, 464 nm, and 536 nm (**1**, **3**, **4** and ligand: $\lambda_{\text{ex}} = 375$ nm, **2**: $\lambda_{\text{ex}} = 466$ nm), respectively. It is known that the emission in Ag(I) complexes is predominantly originated from cluster-centered (MC) or ligand-centered (IL) excited states [32]. In the case of **1**, the maximum emission wavelength ($\lambda_{\text{em}} = 569$ nm) is a little red-shifted compared to the free ligand and is assigned to a ligand-centered (IL) state that is slightly perturbed by the coordination interaction of silver ions [75]. For Zn/Cd complexes, obvious blue-shift and significant enhancement in emission intensity are observed. Because the Zn(II) and Cd(II) ions are difficult to be oxidized or reduced, and there are no d–d transitions with a d¹⁰ closed shell electronic configuration, the emissions of **3** and **4** possibly originate from ligand-centered (LC) and/or ligand-to-ligand charge transfer (LLCT) [76–80]. By sharp contrast, a striking red-shift of the emission is found for **2** that displays an intense low-energy red emission. Time-resolved emission measurements disclosed that the red emission follows a double-exponential decay with a decay lifetime of 1.37 μs ($\lambda_{\text{ex}} = 466$ nm) (Figure 6(b)), which can be assigned as a weak phosphorescence [5, 43, 81, 82]. In general, possible assignments for the excited states which are responsible for emission phenomena of Cu(I)-complexes includes ligand-centered $\pi-\pi^*$ transitions (LC), metal-cluster-centered transitions (CC), ligand-to-ligand (LLCT), ligand-to-metal (LMCT), metal-to-ligand (MLCT) charge transfer transitions or metal centered d¹⁰→d⁹s¹(MC) transitions [43, 83, 84]. In the case of **2**, the emission may be tentatively ascribed to a LMCT band by comparison to the luminescence properties of reported polynuclear Cu(I)-thiolated clusters [40, 69, 85–90].

The photoluminescence properties of **1**, **3**, and **4** are quite common. By contrast, such a low energy emission observed with **2** is rare among the reported metal coordination complexes with heterocyclic thioamides. To our knowledge, there is only one example precedent to our report from Hong's group who reported a red luminescent polymeric cuprous coordination polymer with the pymtH ligand [42]. To better understand the origin of the red emission with **2**, density function theory (DFT) calculations with the ground-state geometries adapted from the X-ray data were performed for **2**. As shown in Figure 7, the LUMO (the

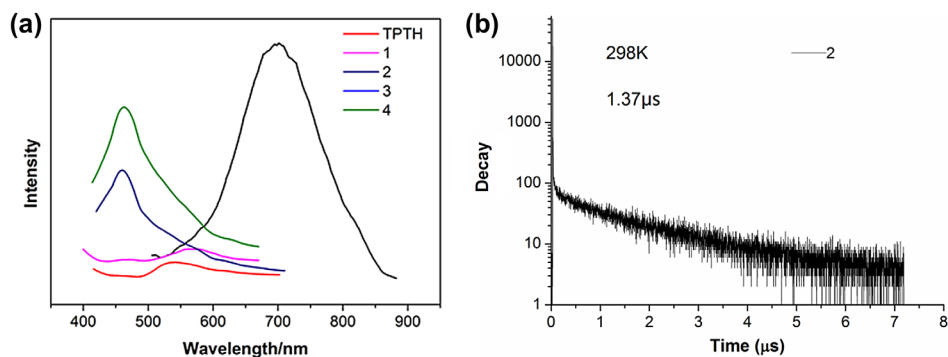


Figure 6. (a) Emission spectra of TPTH and **1–4** in the solid state at room temperature; (b) Emission decay time of **2** (powder).

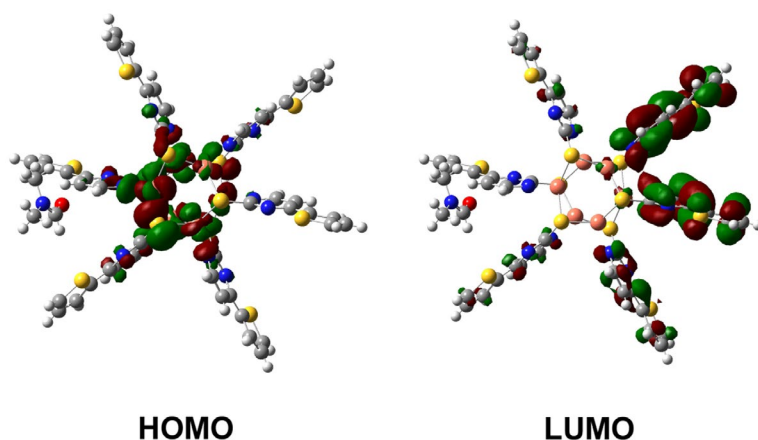


Figure 7. Electron-density distributions of HOMO and LUMO frontier orbitals of **2**.

lowest unoccupied molecular orbital) mainly comprises p-orbitals of C, N and S in TPTH, while the HOMO (the highest occupied molecular orbital) mainly consists of p-orbitals of ligand TPTH as well as d-orbitals of Cu(I) atom. Upon excitation, the electron density has moved from Cu d-orbitals together with TPTH p-orbitals to p-orbitals of C, N, and S. Moreover, the excitation energy is 1.93 eV (or 644.0 nm), which is close to the experimental emission value (1.77 eV or 699 nm). Taken together, it can be concluded that the red emission at 699 nm of **2** originates from a ligand to metal charge transfer.

4. Conclusion

In this article, we describe the synthesis, structural characterization, and photophysical properties of four d^{10} transition-metal complexes with the TPTH (4-(thiophen-2-yl)-pyrimidine-2-thiol) ligand. Under ambient conditions, slow diffusion reactions between TPTH and d^{10} metal ions (Ag^+ , Cu^+ and Cd^{2+}) favor the formation of discrete coordination complexes possibly caused by the steric hindrance of the thiophene substituent. However, a solvothermal reaction between Zn^{2+} and TPTH can thermodynamically lead to a 1-D polymeric chain structure. Seven coordination modes (A–G) of TPTH have been observed in **1–4**. Complex **2** based on Cu(I) atom exhibits a strong red photoluminescence, and the DFT calculations suggest that the red emission of **2** is possibly caused by LMCT transition.

Supplementary material

CCDC 1526027–1526030 contains the supplementary crystallographic data for **1–4**. These data can be obtained free of charge via <https://www.ccdc.cam.ac.uk/conts/retrieving.html>, or from the Cambridge Crystallographic Data Center, 12 Union Road, Cambridge CB2 1EZ, UK; Fax: (+44) 1223 336 033; or E-mail: deposit@ccdc.cam.ac.uk. Supplementary data associated with this article can be found in the online version.

Disclosure statement

No potential conflict of interest was reported by the authors.

Funding

This work was supported by the National Natural Science Foundation of China [grant number 21171036]; Fundamental Research Funds for the Central Universities [grant number 3207047406].

ORCID

Wei Li  <http://orcid.org/0000-0001-7801-3643>

References

- [1] P.D. Akrivos. *Coord. Chem. Rev.*, **213**, 181 (2001).
- [2] L. Li, L. Wei, X. Si, L. Fan, C. Wang, H. Hou. *Inorg. Chim. Acta*, **405**, 279 (2013).
- [3] D.Y. Huang, H.M. Hao, P.F. Yao, X.H. Qin, F.P. Huang, Q. Yu, H.D. Bian. *Polyhedron*, **97**, 260 (2015).
- [4] E. López-Torres, M.A. Mendiola, U.J. Pastor. *Inorg. Chem.*, **45**, 3103 (2006).
- [5] C. Yue, C. Yan, R. Feng, M. Wu, L. Chen, F. Jiang, M. Hong. *Inorg. Chem.*, **48**, 2873 (2009).
- [6] P. Bharati, A. Bharti, P. Nath, S. Kumari, N.K. Singh, M.K. Bharty. *Inorg. Chim. Acta*, **443**, 160 (2016).
- [7] P. Aslanidis, P.J. Cox, A.C. Tsipis. *Dalton Trans.*, **39**, 10238 (2010).
- [8] I. Papazoglou, P.J. Cox, A.G. Papadopoulos, M.P. Sigalas, P. Aslanidis. *Dalton Trans.*, **42**, 2755 (2013).
- [9] R. Sultana, T.S. Lobana, R. Sharma, A. Castineiras, T. Akitsu, K. Yahagi, Y. Aritake. *Inorg. Chim. Acta*, **363**, 3432 (2010).
- [10] H.B. Zhu, Y.Z. Wei, L. Liang. *Polyhedron*, **109**, 53 (2016).
- [11] M. Du, Z.H. Zhang, X.J. Zhao, Q. Xu. *Inorg. Chem.*, **45**, 5785 (2006).
- [12] E.S. Raper. *Coord. Chem. Rev.*, **153**, 199 (1996).
- [13] E.S. Raper. *Coord. Chem. Rev.*, **165**, 475 (1997).
- [14] P.J. Beldon, S. Tominaka, P. Singh, T. Saha Dasgupta, E.G. Bithell, A.K. Cheetham. *Chem. Commun.*, **50**, 3955 (2014).
- [15] A. Gallego, O. Castillo, C.J. Gómez-García, F. Zamora, S. Delgado. *Inorg. Chem.*, **51**, 718 (2012).
- [16] Z.M. Hao, J. Wang, X.M. Zhang. *CrystEngComm*, **12**, 1103 (2010).
- [17] J. Zhang, S. Gao, X.X. Zhang, Z.M. Wang, C.M. Che. *Dalton Trans.*, **41**, 2626 (2012).
- [18] A. Eichhöfer, G. Buth. *Eur. J. Inorg. Chem.*, **2005**, 4160 (2005).
- [19] W.P. Su, R. Cao, M.C. Hong, W.T. Wong, J.X. Lu. *Inorg. Chem. Commun.*, **2**, 241 (1999).
- [20] T.S. Lobana, P. Kaur, A. Kaur, R.J. Butcher. *Z. Anorg. Allg. Chem.*, **638**, 195 (2012).
- [21] A.I. Gallego, O. Castillo, F. Zamora, S. Delgado. *RSC Adv.*, **3**, 18406 (2013).
- [22] R.B. Zhang, Z.J. Li, J.K. Cheng, Y.Y. Qin, J. Zhang, Y.G. Yao. *Cryst. Growth Des.*, **8**, 2562 (2008).
- [23] A. Antiñolo, F. Carrillo-Hermosilla, A.E. Corrochano, R. Fandos, J. Fernández-Baeza, A.M. Rodríguez, M.J. Ruiz, A. Otero. *Organometallics*, **18**, 5219 (1999).
- [24] A.S. Kuzovlev, E.V. Savinkina, V.V. Chernyshev, M.S. Grigoriev, A.N. Volov. *J. Coord. Chem.*, **69**, 508 (2015).
- [25] J.F. Song, Y.Y. Jia, J. Shao, R.S. Zhou, S.Z. Li, X. Zhang. *J. Coord. Chem.*, **69**, 3072 (2016).
- [26] T.N. Mandal, S. Roy, A.K. Barik, S. Gupta, R.J. Butcher, S.K. Kar. *Inorg. Chim. Acta*, **362**, 1315 (2009).
- [27] T.S. Lobana, P. Kaur, G. Hundal, R.J. Butcher, A. Castineiras. *Z. Anorg. Allg. Chem.*, **634**, 747 (2008).
- [28] A. Rodríguez, J.A. García-Vázquez, J. Romero, A. Sousa-Pedrares, A. Sousa, J. Castro. *Z. Anorg. Allg. Chem.*, **633**, 763 (2007).
- [29] H.B. Zhu, G. Xu, J.F. Ji, S.H. Gou. *J. Coord. Chem.*, **62**, 2276 (2009).
- [30] H.B. Zhu, Y.F. Wu, Y. Zhao, J. Hu. *Dalton Trans.*, **43**, 17156 (2014).
- [31] E. Hupf, E. Lork, S. Mebs. *Inorg. Chem.*, **54**, 1847 (2015).
- [32] A. Barbieri, G. Accorsi, N. Armaroli. *Chem. Commun.*, **18**, 2185 (2008).
- [33] K. Matsumoto, T. Shindo, N. Mukasa, T. Tsukuda, T. Tsubomura. *Inorg. Chem.*, **49**, 805 (2010).
- [34] A.L. Johnson, A.M. Willcocks, S.P. Richards. *Inorg. Chem.*, **48**, 8613 (2009).
- [35] S. Budagumpi, S. Endud. *Organometallics*, **32**, 1537 (2013).
- [36] G. Henkel, B. Krebs. *Chem. Rev.*, **104**, 801 (2004).
- [37] J.Y. Corey. *Chem. Rev.*, **111**, 863 (2011).

- [38] S. Budagumpi, A. Haque, S. Endud, G.U. Rehman, A.W. Salman. *Eur. J. Inorg. Chem.*, **2013**, 4367 (2013).
- [39] T. Tsubomura, Y. Ito, S. Inoue, Y. Tanaka, K. Matsumoto, T. Tsukuda. *Inorg. Chem.*, **47**, 481 (2008).
- [40] P.J. Barnard, L.E. Wedlock, M.V. Baker, S.J. Berners-Price, D.A. Joyce, B.W. Skelton, J.H. Steer. *Angew. Chem. Int. Ed. Engl.*, **45**, 5966 (2006).
- [41] G.K. Patra, P.K. Pal, J. Mondal, A. Ghorai, A. Mukherjee, R. Saha, H.K. Fun. *Inorg. Chim. Acta*, **447**, 77 (2016).
- [42] L. Han, M. Hong, R. Wang, B. Wu, Y. Xu, B. Lou, Z. Lin. *Chem. Commun.*, **22**, 2578 (2004).
- [43] G. Christofidis, P.J. Cox, P. Aslanidis. *Polyhedron*, **31**, 502 (2012).
- [44] A. Austin, G. Petersson, M.J. Frisch, F.J. Dobek, G. Scalmani, K. Throssell. *J. Chem. Theory Comput.*, **8**, 4989 (2012).
- [45] Gaussian 09, Revision D.01, M.J. Frisch, G.W. Trucks, H.B. Schlegel, G.E. Scuseria, M.A. Robb, J.R. Cheeseman, G. Scalmani, V. Barone, B. Mennucci, G.A. Petersson, H. Nakatsuji, M. Caricato, X. Li, H.P. Hratchian, A.F. Izmaylov, J. Bloino, G. Zheng, J.L. Sonnenberg, M. Hada, M. Ehara, K. Toyota, R. Fukuda, J. Hasegawa, M. Ishida, T. Nakajima, Y. Honda, O. Kitao, H. Nakai, T. Vreven, J.A. Montgomery Jr, J.E. Peralta, F. Ogliaro, M. Bearpark, J.J. Heyd, E. Brothers, K.N. Kudin, V.N. Staroverov, R. Kobayashi, J. Normand, K. Raghavachari, A. Rendell, J.C. Burant, S.S. Iyengar, J. Tomasi, M. Cossi, N. Rega, J.M. Millam, M. Klene, J.E. Knox, J.B. Cross, V. Bakken, C. Adamo, J. Jaramillo, R. Gomperts, R.E. Stratmann, O. Yazyev, A.J. Austin, R. Cammi, C. Pomelli, J.W. Ochterski, R.L. Martin, K. Morokuma, V.G. Zakrzewski, G.A. Voth, P. Salvador, J.J. Dannenberg, S. Dapprich, A.D. Daniels, Ö. Farkas, J.B. Foresman, J.V. Ortiz, J. Cioslowski, D.J. Fox. *Gaussian Inc.*, Wallingford, CT (2009).
- [46] *SAINT (Version 6.02a)*, Bruker AXS Inc., Madison, WI (2002).
- [47] G.M. Sheldrick. *SADABS, Program for Bruker Area Detector Absorption Correction*, University of Göttingen, Germany (1997).
- [48] G.M. Sheldrick. *Acta Crystallogr., Sect. A: Found. Crystallogr.*, **64**, 112 (2008).
- [49] H.B. Zhu, L. Li, G. Xu, S.H. Gou. *Eur. J. Inorg. Chem.*, **2010**, 1143 (2010).
- [50] H.B. Zhu, S.Y. Zhang, X. Lu, W.N. Yang, S.H. Gou, J. Chen. *Z. Anorg. Allg. Chem.*, **637**, 1423 (2011).
- [51] H.B. Zhu, R.Y. Shan, W.N. Yang, S.H. Gou. *Z. Anorg. Allg. Chem.*, **639**, 125 (2013).
- [52] M. Hong, W. Su, R. Cao, W. Zhang. *Inorg. Chem.*, **38**, 600 (1999).
- [53] L. Han, Z. Chen, J. Luo, M. Hong, R. Cao. *Acta Crystallogr., Sect. E: Cryst. Struct. Commun.*, **58**, 383 (2002).
- [54] W. Su, R. Cao, M. Hong, W. Wong. *Inorg. Chem. Commun.*, **2**, 241 (1999).
- [55] W.P. Su, M.C. Hong, J.B. Weng, Y.C. Liang, Y.J. Zhao, R. Cao, Z.Y. Zhou, A.S.C. Chan. *Inorg. Chim. Acta*, **331**, 8 (2002).
- [56] C. Yan, L. Chen, R. Feng, F. Jiang, M. Hong. *CrystEngComm.*, **11**, 2529 (2009).
- [57] A. Beheshti, W. Clegg, R. Khorramdin, V. Nobakht, L. Russo. *Dalton Trans.*, **40**, 2815 (2011).
- [58] A. Gallego, O. Castillo, C.J. Gómez-García, F. Zamora, S. Delgado. *Eur. J. Inorg. Chem.*, **2014**, 3879 (2014).
- [59] C.H. Huang, S.H. Gou, H.B. Zhu, W. Huang. *Inorg. Chem.*, **46**, 5537 (2007).
- [60] Z.M. Hao, X.M. Zhang. *Cryst. Growth Des.*, **8**, 2359 (2008).
- [61] I. Kinoshita, L.J. Wright, S. Kubo, K. Kimura, A. Sakata, T. Yano, R. Miyamoto, T. Nishioka, K. Isobe. *Dalton Trans.*, **153**, 1993 (2003).
- [62] S.S. Lemos, M.A. Camargo, Z.Z. Cardoso, V.M. Deflon, F.H. Försterling, A. Hagenbach. *Polyhedron*, **20**, 849 (2001).
- [63] T.S. Lobana, R. Verma, G. Hundal, A. Castineiras. *Polyhedron*, **19**, 899 (2000).
- [64] R. Castro, J. Romero, J.A. Garcia-Vazquez, A. Sousa, Y.D. Chang. *Inorg. Chim. Acta*, **245**, 119 (1996).
- [65] L. Han, X. Bu, Q. Zhang, P. Feng. *Inorg. Chem.*, **45**, 5736 (2006).
- [66] J. Wang, Y.H. Zhang, H.X. Li, Z.J. Lin, M.L. Tong. *Cryst. Growth Des.*, **7**, 2352 (2007).
- [67] K. Singh, J.R. Long, P. Stavropoulos. *J. Am. Chem. Soc.*, **119**, 2942 (1997).
- [68] S. Seth, A.K. Das, T.C.W. Mak. *Acta Crystallogr., Sect. C: Cryst. Struct. Commun.*, **51**, 2529 (1995).
- [69] M.J. Zhang, H.X. Li, H.Y. Li, J.P. Lang. *Dalton Trans.*, **45**, 17759 (2016).
- [70] H.Y. Xie, I. Kinoshita, T. Karasawa, K. Kimura, T. Nishioka, I. Akai, K. Kanemoto. *J. Phys. Chem. B*, **109**, 9339 (2005).

- [71] R. Castro, M.L. Durán, J.A. García-Vázquez, J. Romero, A. Sousa, E.E. Castellano, J. Zukerman-Schpector. *J. Chem. Soc., Dalton Trans.*, **23**, 2559 (1992).
- [72] C. Yue, C. Yan, R. Feng, M. Wu, L. Chen, F. Jiang, M. Hong. *Inorg. Chem.*, **48**, 2873 (2009).
- [73] E. Block, M. Gernon, H.Y. Kang. *Angew. Chem. Int. Ed. Engl.*, **27**, 1342 (1988).
- [74] A. Rodríguez, A. Sousa-Pedrares, J.A. García-Vázquez, J. Romero, A. Sousa. *Eur. J. Inorg. Chem.*, **2011**, 3403 (2011).
- [75] G. Christofidis, P.J. Cox, P. Aslanidis. *Polyhedron*, **31**, 502 (2012).
- [76] L. Fan, L. Li, B. Xu, M. Qiao, J. Li, H. Hou. *Inorg. Chim. Acta*, **423**, 46 (2014).
- [77] R.Y. Huang, H. Jiang, C.H. Zhu, H. Xu. *RSC Adv.*, **6**, 3341 (2016).
- [78] X. Chen, B. Zhang, F. Yu, M. Su, W. Qin, B. Li, G. Zhuang, T. Zhang. *CrystEngComm.*, **18**, 6396 (2016).
- [79] G. Li, G. Liu, L. Xin, X. Li, L. Ma, L. Wang. *J. Inorg. Organomet. Polym.*, **25**, 694 (2015).
- [80] X. Li, B.L. Wu, C.Y. Niu, Y.Y. Niu, H.Y. Zhang. *Cryst. Growth Des.*, **9**, 3423 (2009).
- [81] D.P. Jiang, R.X. Yao, F. Ji, X.M. Zhang. *Eur. J. Inorg. Chem.*, **2013**, 556 (2013).
- [82] I.S. Krytchankou, I.O. Koshevoy, V.V. Gurzhiy, V.A. Pomogaev, S.P. Tunik. *Inorg. Chem.*, **54**, 8288 (2015).
- [83] C. Tard, S. Perruchas, S. Maron, X.F. Le Goff, F. Guillen, A. Garcia, J. Vigneron, A. Etcheberry, T. Gacoin, J.P. Boilot. *Chem. Mater.*, **20**, 7010 (2008).
- [84] T.H. Kim, Y.W. Shin, J.H. Jung, J.S. Kim. *Angew. Chem. Int. Ed.*, **47**, 685 (2008).
- [85] C.K. Ryu, M. Vitale, P.C. Ford. *Inorg. Chem.*, **32**, 869 (1993).
- [86] K.R. Kyle, C.K. Ryu, J.A. Dibeneditto, P.C. Ford. *J. Am. Chem. Soc.*, **113**, 2954 (1991).
- [87] J.K. Cheng, Y.B. Chen, L. Wu, J. Zhang, Y.H. Wen, Z.J. Li, Y.G. Yao. *Inorg. Chem.*, **44**, 3386 (2005).
- [88] R. Langer, M. Yadav, B. Weinert, D. Fenske, O. Fuhr. *Eur. J. Inorg. Chem.*, **2013**, 3623 (2013).
- [89] H. Zhou, P. Lin, Z.H. Li, S.W. Du. *J. Mol. Struct.*, **881**, 21 (2008).
- [90] X.C. Shan, F.L. Jiang, D.Q. Yuan, M.Y. Wu, S.Q. Zhang, M.C. Hong. *Dalton Trans.*, **41**, 9411 (2012).